SCIENCE CHINA
Earth Sciences

•ARTICLE•

September 2025 Vol.68 No.9: 3064–3076
https://doi.org/10.1007/s11430-025-1647-y

Depth-dependent accumulation and controls of particulate and mineral-associated organic carbon in Inner Mongolian grasslands

Haojun ZHENG[1†], Shuai ZHANG[2†], Guocheng WANG[1*], Mingming WANG[2], Yunlong HU[3], Yuchen WEI[2], Kang XU[2], Haigang LI[4], Shixiang ZHAO[4], Biao ZHU[3], Jinfeng CHANG[2], Zhou SHI[2], Su YE[2], Changqing SONG[1], Wen ZHANG[5] & Zhongkui LUO[2*]

[1] *State Key Laboratory of Earth Surface Processes and Disaster Risk Reduction, Faculty of Geographical Science, Beijing Normal University, Beijing 100875, China*
[2] *State Key Laboratory of Soil Pollution Control and Safety, College of Environment and Resource Sciences, Zhejiang University, Hangzhou 310058, China*
[3] *Institute of Ecology, College of Urban and Environmental Sciences, and Key Laboratory for Earth Surface Processes of the Ministry of Education, Peking University, Beijing 100871, China*
[4] *Inner Mongolia Key Laboratory of Soil Quality and Nutrient Resources, College of Resources and Environmental Sciences, Inner Mongolia Agricultural University, Hohhot 010018, China*
[5] *State Key Laboratory of Atmospheric Boundary Layer Physics and Atmospheric Chemistry, Institute of Atmospheric Physics, Chinese Academy of Sciences, Beijing 100029, China*

Received February 7, 2025; revised June 25, 2025; accepted July 21, 2025; published online August 19, 2025

Abstract Global grasslands can sequester soil organic carbon (SOC) while maintaining ecosystem function, thereby mitigating climate change. SOC consists of components with varying stability and turnover rates, such as particulate organic carbon (POC) and mineral-associated organic carbon (MAOC). While these components have been extensively studied in the surface layer (0–30 cm), their distribution and controls in deeper layers remain poorly understood. This study combined precise measurements of POC and MAOC across seven sequential depth layers down to 2 m at 17 Inner Mongolian grassland sites with a global dataset to elucidate their vertical distribution patterns and underlying controls. Results showed that POC generally dominated MAOC in Inner Mongolian grassland soils, albeit with regional variations in this dominance. Interestingly, the proportion of MAOC to total SOC (MAOC:(MAOC+POC)), indicating SOC stability, increased with depth in the upper 0–50 cm but decreased below 50 cm, suggesting that environmental factors at depth may constrain POC decomposition and MAOC formation. POC accumulation was positively influenced by the mean annual precipitation in the top 30 cm and negatively affected by soil pH down to 50 cm. Contrastingly, MAOC was coregulated by the clay and silt content (CS) and aluminum (Al) oxide in surface soils (0–30 cm), whereas Al oxide dominated from 30 to 100 cm. Notably, MAOC:(MAOC+POC) correlated significantly with CS across all depths, underscoring the persistent role of physical protection mechanisms in deeper layers. These findings highlight depth-specific accumulation patterns and controls of POC and MAOC in the Inner Mongolian grasslands, indicating that optimizing SOC sequestration under changing climate and management scenarios requires depth-specific strategies that target both short-term POC enhancement and long-term MAOC stabilization.

Keywords Soil organic carbon, Inner Mongolian grasslands, POC, MAOC, Depth distribution

Citation: Zheng H, Zhang S, Wang G, Wang M, Hu Y, Wei Y, Xu K, Li H, Zhao S, Zhu B, Chang J, Shi Z, Ye S, Song C, Zhang W, Luo Z. 2025. Depth-dependent accumulation and controls of particulate and mineral-associated organic carbon in Inner Mongolian grasslands. Science China Earth Sciences, 68(9): 3064–3076, https://doi.org/10.1007/s11430-025-1647-y

† These authors contributed equally to this work.
* Corresponding authors: Guocheng WANG (wanggc@bnu.edu.cn), Zhongkui LUO (luozk@zju.edu.cn)

1. Introduction

Grasslands, the most widespread terrestrial ecosystem, play a crucial role in the global carbon cycle (Bai and Cotrufo, 2022; Liu et al., 2023). They store substantial amounts of carbon, of which approximately 90% is stored belowground primarily as soil organic carbon (SOC), which is highly susceptible to changes in climate and land use (Bai and Cotrufo, 2022; Zheng et al., 2024a). Due to their vast extent, global grasslands hold 343 Pg (1 Pg=1×10^{15} g) of organic carbon within the top 1 m of soil, accounting for about one-fifth of terrestrial SOC stocks (Dondini et al., 2023). While most research has focused on surface soils up to a depth of 30 cm, deeper soil layers represent an important yet often overlooked carbon pool (Jobbágy and Jackson, 2000; Henneron et al., 2022). Although SOC concentrations are generally lower in subsoil layers compared with topsoil layers, subsoils store considerable carbon due to their greater volume and exhibit much slower decomposition rates, implying a greater potential for long-term carbon sequestration (Schiedung et al., 2023). Therefore, revealing the behavior of SOC accumulation at different soil depths and identifying their controlling factors are vital for enhancing carbon sequestration and sustaining the ecological services provided by grasslands under changing climatic conditions.

SOC comprises numerous organic compounds with diverse origins, chemical structures, and persistence (Luo et al., 2020; Sokol et al., 2022; Sun et al., 2023). These compounds can be broadly categorized into two functionally distinct fractions: particulate organic carbon (POC) and mineral-associated organic carbon (MAOC) (Cotrufo et al., 2019; Lavallee et al., 2020). POC primarily arises from the fragmentation of plant and microbial residues and consists of large polymers. In contrast, MAOC is derived from smaller molecules leached from plant residues or exuded by plant roots, which either directly associate with minerals (*ex vivo*) or are incorporated into soil through microbial assimilation (*in vivo*) as microbial necromass (Liang et al., 2017; Sokol et al., 2019). Generally, MAOC has a longer transit time than POC does and is less sensitive to climate change (Cotrufo et al., 2019; Rocci et al., 2021), largely because of its strong chemical bonds with soil minerals and physical protection by fine aggregates (Tang et al., 2024). Consequently, the proportion of MAOC to total SOC (MAOC:(MAOC+POC)) can indicate the stability of SOC to climate change, making MAOC a key component for long-term SOC sequestration (Lavallee et al., 2020; Begill et al., 2023).

The accumulation dynamics of POC and MAOC in topsoil (typically 0–30 cm depth) have been extensively studied (Briedis et al., 2012; Rocci et al., 2021). Topsoil POC is widely recognized to be predominantly controlled by carbon inputs, increasing linearly or even exponentially with total SOC, thereby making POC the dominant fraction in SOC-rich soils (Cotrufo et al., 2019; Estop-Aragonés et al., 2020). Conversely, MAOC accumulation requires binding sites, which are primarily determined by the abundance of fine soil particles (i.e., clay and silt). Once these binding sites become saturated, additional organic carbon is less likely to be stabilized as free MAOC, which is more readily utilized by microbes (Cotrufo et al., 2019).

However, deeper soil layers exhibit biogeochemical characteristics that differ markedly from those of topsoil, including lower oxygen availability, reduced microbial activity, and shifts in organic matter input sources (Bernal et al., 2016). These unique conditions may support distinct accumulation and transformation mechanisms of POC and MAOC, potentially leading to depth-specific carbon stabilization pathways. In a recent global analysis of soils at 0–100 cm depth, Zhou et al. (2024) found that POC exhibits a shallower vertical distribution than MAOC, and that warming significantly accelerates the decomposition of both fractions in deeper soil layers. These results are consistent with other studies showing that deep soil carbon is as sensitive-or even more sensitive-to warming than topsoil carbon (Hicks Pries et al., 2017; Button et al., 2022). Despite these advances, field observation data directly measuring different carbon components in deep soil remain scarce, limiting our ability to generalize findings or predict deep soil carbon response to global change. To elucidate the mechanisms controlling the vertical distribution and accumulation of these SOC fractions, comprehensive datasets spanning the entire soil profile are essential. Such data will improve mechanistic understanding of SOC dynamics and inform strategies for whole-profile carbon sequestration.

In this study, we sampled soil profiles down to 2 m at 17 sites across the Inner Mongolian grasslands, which are a major component of the Eurasian Steppe (Figure 1), and we measured MAOC and POC across seven sequential depths. We tested the hypothesis that MAOC is more dominant in deeper soil layers because deep soil receives carbon primarily through root deposition, dissolved carbon from upper layers, and microbial necromass, which can directly contribute to MAOC formation (Sokol et al., 2019; Hicks Pries et al., 2023). For this reason, deeper soil layers should present higher MAOC:(MAOC+POC) ratios, with MAOC increasing more rapidly in deeper layers as the SOC content increases. In addition, we measured and collected a comprehensive set of environmental covariates, including bioclimatic conditions, edaphic properties, terrain conditions, livestock density, and vegetation dynamics. We aimed to address the following questions: (1) What are the vertical distribution patterns of POC and MAOC across the whole soil profile in the Inner Mongolian grasslands? (2) How do the effects of climatic and edaphic variables vary with soil depth? Answering these questions is crucial for advancing our understanding of SOC accumulation and stabilization

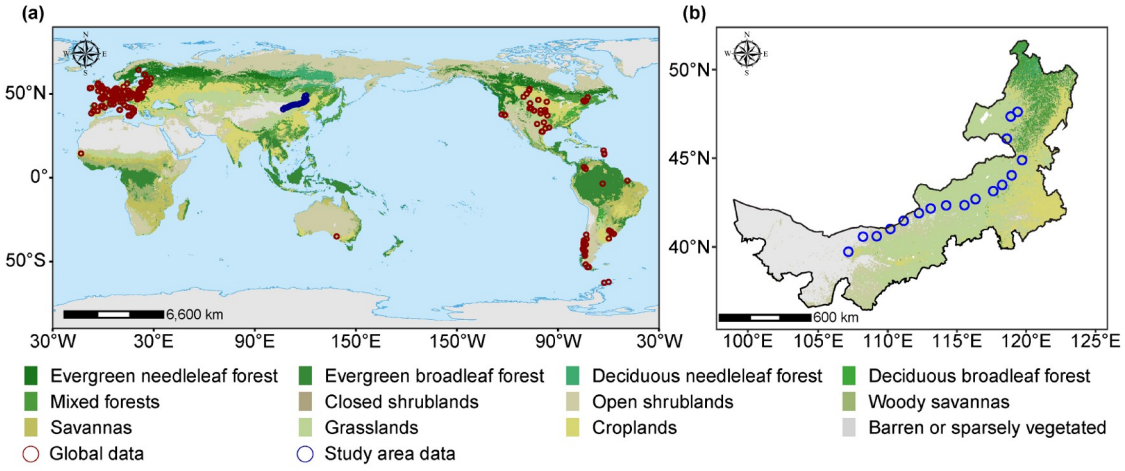

Figure 1 Locations of sampled grassland soil profiles globally (a) and in the study area (b). Blue circles represent data from soils sampled and measured in the study area. Red circles denote data of global temperate grasslands sourced from a data synthesis study reported by Georgiou et al. (2022).

mechanisms across soil depths, and for informing the development of whole-profile strategies to optimize SOC sequestration under changing climate conditions and land management regimes.

2. Materials and methods

2.1 Whole-soil profile sampling across the Inner Mongolian grasslands

The Inner Mongolian grasslands are characterized primarily by a temperate climate. On average, the mean annual temperature (MAT) increases from northeast to southwest, ranging from −1.8°C to 7.7°C, while mean annual precipitation (MAP) decreases along the same gradient, ranging from 415 to 179 mm (Wang et al., 2022a). These grasslands can be broadly classified into three major types: meadow steppe, typical steppe, and desert steppe (Wang G C et al., 2021, 2022b). The meadow steppe is predominantly distributed in the eastern areas, the typical steppe is mainly located in central Inner Mongolia, and the desert steppe is found primarily to the west of the typical steppe (Figure 1).

During July–August 2020, soil cores were collected at 17 sites, which extended from northeast to southwest and covered the three main grassland types (Figure 1). The soil cores, which were collected down to a depth of 2 m, comprised seven layers (0–10, 10–20, 20–30, 30–50, 50–100, 100–150, and 150–200 cm). Three 10 m×10 m sampling quadrats were established at each site as three replicates. Five randomized soil profiles were collected and combined within each quadrat to form a composite sample on the basis of depth. These soil samples were stored in airtight polypropylene bags and transported to the laboratory in a cooler with ice cubes. The soil samples were sieved to 2 mm in the laboratory to remove stones and visible roots.

2.2 Measurements of soil C, its components, and other physical and chemical properties

SOC was analyzed using an elemental analyzer (EA 3000, Euro Vector, Italy). Prior to the analysis, air-dried soil samples were treated with 0.1 mol L^{-1} hydrochloric acid to remove carbonates, rinsed with deionized water, air-dried, and passed through a 0.149 μm sieve (Harris et al., 2001). The soil pH was measured in a 1:2.5 soil-to-water suspension using a pH electrode (Mettler-Toledo, Switzerland). The soil texture was analyzed using a laser particle size analyzer (LS-CWM, OMEC, China) after full dispersion of the air-dried soil sample with hydrochloric acid and then hydrogen peroxide to remove carbonate and organic matter (Minasny and McBratney, 2001). Free iron (Fe) and aluminum (Al) oxides in soil were extracted using the dithionite-citrate-bicarbonate (DCB) method (Collignon et al., 2012). The soil exchangeable calcium (Ca) and magnesium (Mg) were extracted at a 1:25 soil-to-solution ratio with 50 mL of 1 mol L^{-1} ammonium acetate solution (Ciesielski et al., 1997). The extracts were analyzed for Fe, Al, Ca, and Mg contents using inductively coupled plasma-optical emission spectrometry (ICP-OES) (Perkin Elmer, Optima 7000 DV, USA). The soil bulk density was measured by drying a 100 cm^3 cutting ring at 105°C for 48 h.

POC and MAOC were separated from bulk soil using the wet sieving and fractionation methods (Six et al., 2001). Briefly, 10 g of bulk soil was dispersed in 50 mL of 5 g L^{-1} sodium hexametaphosphate solution by shaking for 18 h. Next, the soil samples were completely washed on a sieve (53 μm) with deionized water. The carbon in soil particles retained on the 53 μm sieve (>53 μm) was considered POC, and the carbon in material that passed through the sieve (<53 μm) was considered MAOC. Both the POC and MAOC samples were dried at 60°C. Afterward, the organic carbon

content of the dried samples was analyzed via an elemental analyzer (EA 3000, Euro Vector, Italy) according to the method of SOC measurement described above. The final POC and MAOC contents were calculated on the basis of the recovered mass. The final soil mass recovery rate was greater than 97% for all samples. In addition to individual POC and MAOC, we calculated the ratio of MAOC to SOC, i.e., MAOC:(MAOC+POC), to indicate SOC stability.

2.3 Environmental and anthropogenic covariates

Focusing on POC, MAOC, and MAOC:(MAOC+POC), we aimed to investigate their depth and spatial distributions and evaluate how they correlate with various environmental drivers. In addition to the measured soil properties (see Sections 2.1 and 2.2), we compiled an additional set of environmental and anthropogenic variables. These variables include the mean climate variables, terrain variables, remote sensing variables, vegetation variables, and human disturbance variables (Table S1). Further details are elaborated below.

The mean climate data, with a spatial resolution of 30 arc seconds, were sourced from WorldClim2 (www.worldclim.org). The dataset includes eleven temperature-related and eight precipitation-related variables (Bio1–Bio19; Table S2) that quantify biologically meaningful variables using monthly maximum and minimum temperature and precipitation (Fick and Hijmans, 2017). We acquired 16 terrain variables from a global gridded dataset with a spatial resolution of 30 arc seconds (Amatulli et al., 2018). This comprehensive set of terrain variables includes elevation, roughness, the terrain ruggedness index, the topographic position index, the vector ruggedness measure, aspect, landform, slope, indices indicating both east-west and north-facing aspects of a site, profile curvature, tangential curvature, and first- and second-order partial derivatives for both east-west and north-south slopes, providing a detailed representation of the terrain conditions.

We extracted the Moderate Resolution Imaging Spectroradiometer (MODIS) net primary productivity (NPP) from a global gridded dataset with a spatial resolution of 500 m (Zhao et al., 2005). Following Wang G C et al. (2021), grazing intensity was quantified based on the population of three key livestock species (cattle, goats, and sheep), as they constitute the majority of livestock in the Inner Mongolian grasslands (Table S1). The grazing intensity data at a 10 km spatial resolution were obtained from Gilbert et al. (2018).

2.4 Landsat-based seasonality amplitude

We retrieved multispectral seasonality amplitudes (Table S3) from Landsat-based time series to capture vegetation dynamics in historical periods. All available Landsat 5, 7, 8, and 9 observations were downloaded from the Google Earth Engine platform on a per-sample basis. We screened out the cloud, shadow, and snow pixels indicated by the Landsat quality assessment bands generated by the Fmask algorithm (Zhu and Woodcock, 2012). Then, we applied continuous change detection and classification (CCDC, Zhu et al., 2020) to segment each sample-based time series by detecting its spectral breaks. Each segment represents a historical period during which the land cover has stable spectral characteristics. For each sample, we selected the temporal segment in which the fieldwork date occurred and then used the harmonic model to fit all Landsat observations for the selected segment. The harmonic model was denoted as follows:

$$\hat{\rho}_{i,x} = c_{0,i} + \sum_{k=1}^{3}\left\{a_{k,i}\cos(2\pi kx / T + \varphi)\right\} + c_{1,i}x,$$

where x is the Julian date, i is the ith Landsat band (i=1, 2, …, 7), k is the temporal frequency of the harmonic component, T is the number of days per year (T=365.25), $c_{0,i}$ is the intercept, $c_{1,i}$ is the slope, φ is the phase, and $a_{k,j}$ is the seasonality amplitude (k=1, 2, and 3). Three amplitude coefficients were extracted for each Landsat band, forming 21 amplitude coefficients, representing a comprehensive set of vegetation properties.

2.5 Assessment of drivers of POC, MAOC, and MAOC:(MAOC+POC)

We hypothesized that the two dependent variables (POC and MAOC) could be influenced by various environmental and anthropogenic factors (Liu M L et al., 2025). These factors include the mean climate variables, soil properties, terrain attributes, Landsat-based time-series coefficients of vegetation dynamics, vegetation and human disturbance variables (Table S1), and soil depth. To facilitate interpretation, we utilized redundancy analysis (RDA) to explore the connections between the variables and the three response variables (POC, MAOC, and MAOC:(MAOC+POC)) (Legendre and Legendre, 1988; Wagner, 2004). Prior to RDA, we conducted detrended correspondence analysis (DCA) on the response variable matrix, which yielded a compositional gradient length of 1.76, indicating that RDA was appropriate for the dataset since this value is less than 3 (Ter Braak and Prentice, 1988). All the variables were standardized to eliminate unit arbitrariness, ensuring comparability among the canonical coefficients (González et al., 1998). To avoid multicollinearity, variables were selected by the variance inflation factor (VIF), which quantifies the severity of multicollinearity in regression analysis, and those with VIF exceeding 10 were excluded (Akinwande et al., 2015). The final selected variables are listed in Table S4. Furthermore, a hierarchical partitioning (HP) method was used to identify the relative contributions of a variable to the explained variance of the three SOC variables (Lai et al., 2022). The RDA

and HP were conducted using the vegan and rdacca.hp R packages within the R environment (R Core Team, 2024).

We further explored the direct and indirect effects of external factors on POC, MAOC, and MAOC:(MAOC+POC) by implementing a path model (i.e., structural equation model). Five latent variables and their corresponding manifest variables were incorporated into the path model: climate (represented by mean annual precipitation (MAP)), terrain (represented by altitude), human disturbance (represented by grazing intensity (GI), with all animals, including sheep, goats, and cattle, converted to animal units), edaphic attributes (represented by clay and silt content (CS), soil pH, and soil Al oxide), and soil depth. Notably, remote sensing variables were excluded from the model because of their small contributions to model performance. We explored the following potential pathways in a hypothesis-driven path model. First, we assumed that all five latent variables have direct impacts on the POC, MAOC, and MAOC:(MAOC+POC). Second, we postulated that terrain indirectly influences the three dependent variables through its influence on the remaining latent variables, except for soil depth. Third, we proposed that climate indirectly affects the three dependent variables through its influence on other latent variables, except for terrain and soil depth. Four, we assumed that human disturbance indirectly affects the three dependent variables through its influence on edaphic attributes. Finally, we asserted that soil depth indirectly affects the three dependent variables through its impact on edaphic attributes. The partial least squares approach was used to fit the path model, and all the indicators were standardized. Path analyses were conducted using the plspm package in R (R Core Team, 2024).

We also employed Bayesian linear mixed-effects models (BLMMs) to assess the individual responses of the three dependent variables to the major driving factors identified in the RDA with relatively high contributions via the R package brms (R Core Team, 2024). Soil depth was used as a random effect in all the models. Four sampling chains were run for 2,000 iterations, with a warm-up period of 1,000 iterations, resulting in 4,000 total postwarm-up draws. We used the default priors of the brms package, namely, a Student's t distribution for the intercept and weakly informative normal priors for other regression coefficients. Model convergence was assessed using the Rhat statistic implemented in the pp_check function. An Rhat value closer to 1 indicates better convergence of the fitted model. The coefficient of determination (R^2) was calculated based on the posterior predictive distribution using the bayes_R2 function.

3. Results

Averaged across the 17 sites, both the POC and MAOC concentrations decreased with depth, although MAOC presented a much slower rate of decrease (Figure 2a). The average POC concentrations were 10.90, 7.09, 4.95, 2.93, 1.90, 1.06, and 0.95 g C kg^{-1} in the 0–10, 10–20, 20–30, 30–50, 50–100, 100–150, and 150–200 cm depth intervals, respectively (Figure 2a). Across the sites, POC varied widely, particularly in the upper layers. In the 0–10 cm depth interval, for example, POC values ranged from 0.76 to 32.80 g C kg^{-1}, while its range narrowed to 0.04–

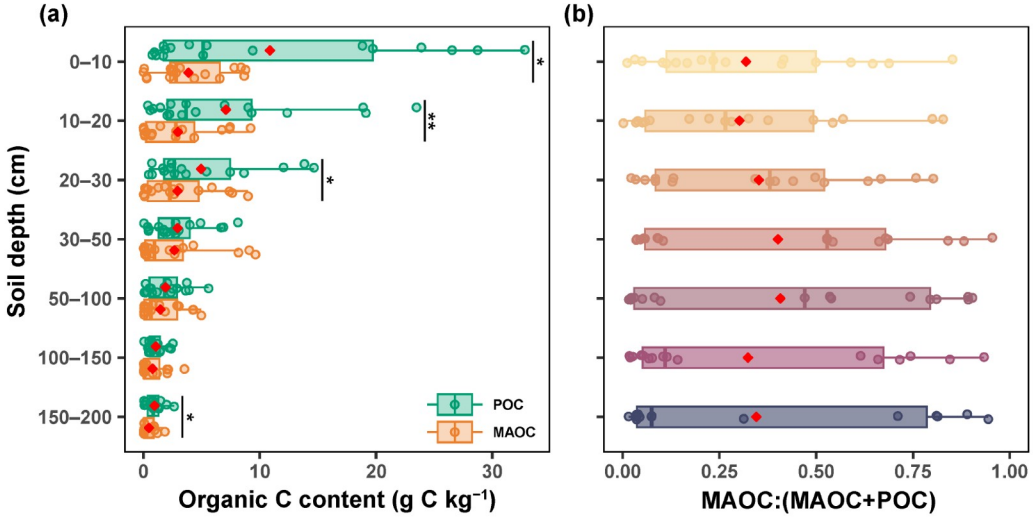

Figure 2 Depth distributions of particulate organic carbon (POC) and mineral-associated organic carbon (MAOC) (a), and the proportion of MAOC to total soil organic carbon (MAOC:(MAOC+POC)) (b) among different soil layers in the grasslands of the study area. The number of samples for each soil depth is as follows: 17 for 0–10, 10–20, 20–30, 30–50, and 50–100 cm; 16 for 100–150 cm; and 14 for 150–200 cm. Box plots represent the 1st and 3rd quartiles (box), medians (central horizontal line), means (red diamond), largest value smaller than 1.5 times the interquartile range (upper vertical line), and smallest value larger than 1.5 times the interquartile range (lower vertical line). Nonparametric paired Wilcoxon signed-rank tests were employed. Significance levels: *, p<0.05; **, p<0.01; ***, p<0.001; no label means no significance. p-values for two-tailed tests.

2.63 g C kg^{-1} in the 150–200 cm depth interval. Compared with those of POC, MAOC concentrations were generally less variable across the 17 sites (Figure 2a). On average, the MAOC concentrations were 3.87, 2.96, 2.93, 2.66, 1.45, 0.78, and 0.48 g C kg^{-1} at the seven soil depths, respectively (Figure 2a). For the proportion of MAOC to SOC (i.e., MAOC:(MAOC+POC)), which is an indicator of SOC stability, no apparent vertical gradients were observed along the soil profile (Figure 2b). In the 0–10, 10–20, and 20–30 cm layers, for example, it ranged from 0.30 to 0.35, on average. At depths of 30–50 and 50–100 cm, the values increased to averages of 0.40 and 0.41, respectively. In the 100–150 and 150–200 cm layers, the values decreased to averages of 0.32 and 0.35, respectively. Despite these vertical variations, MAOC:(MAOC+POC) was not significantly different (p>0.05) among the depth layers.

Averaged across the soil depths, both POC and MAOC increased with SOC, but the slope was steeper for POC in the grasslands of the study area (Figure 3a, 3b). This indicates that more carbon was stored as POC for a unit increase in SOC. Consequently, POC became more dominant than MAOC as total SOC increased in the Inner Mongolian grasslands. This pattern contrasts with the results based on data from the 0–30 cm depth interval in global temperate grasslands (Figure 3c, 3d). Among the soil depths, the slope of the increase in POC was much steeper in the upper layers, such as the 0–10 and 10–20 cm layers, whereas in the middle layers (e.g., 30–50 cm), the slope was gentler (Figure 3a). As a result, more carbon was stored as POC in the upper layers per unit increase in SOC. The increasing slope for MAOC showed the opposite pattern to that of POC (Figure 3b). This pattern is generally consistent with the results based on the global grassland dataset (Figure 3d). Interestingly, the contribution of MAOC to SOC per unit increase in SOC did not linearly increase with soil depth, but reached a tipping point in the 30–50 cm depth interval (Figure 3b). Beyond this tipping point, the contribution of MAOC decreased again.

RDA revealed nine primary factors explaining 58% of the

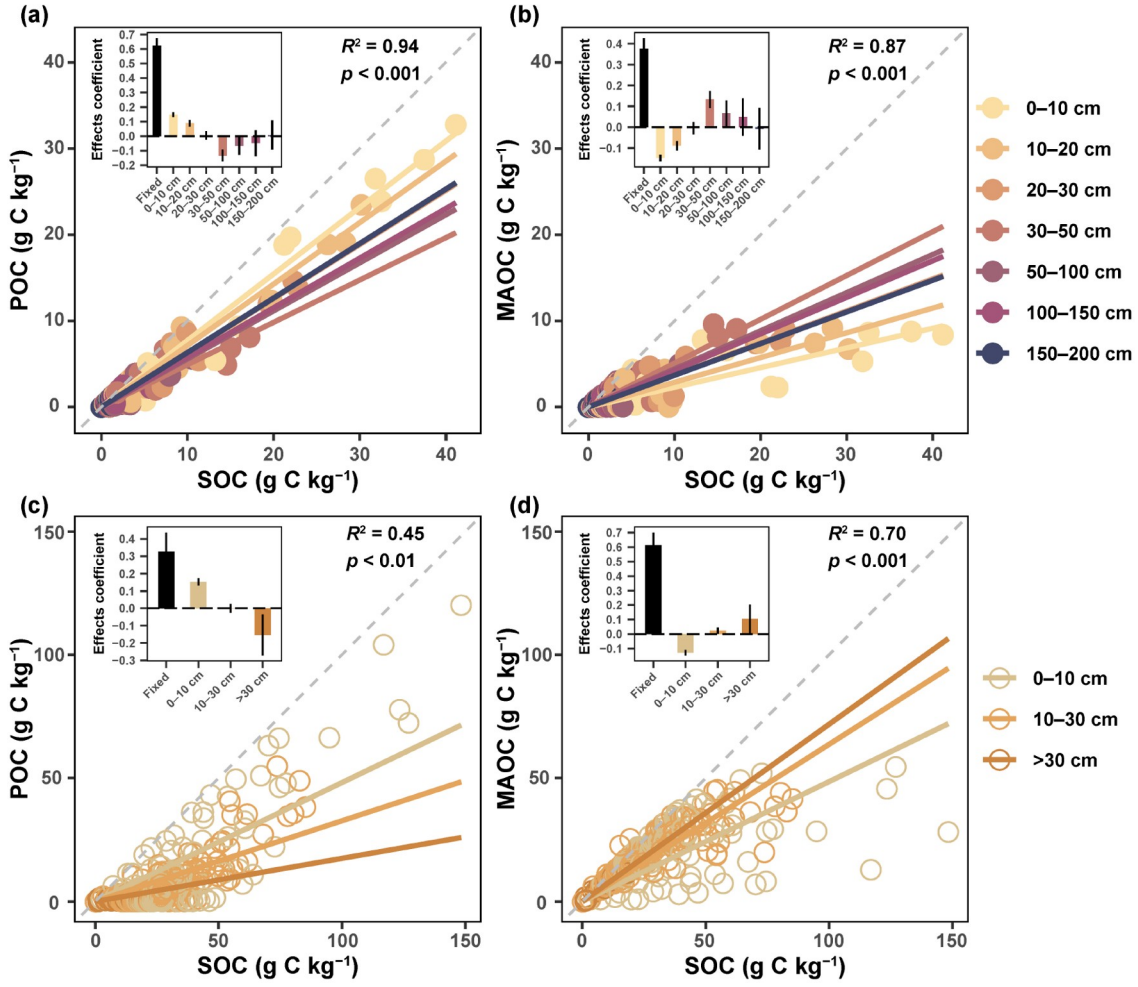

Figure 3 Linear mixed-effects modeling of the relationships between particulate organic carbon (POC) and soil organic carbon (SOC), and mineral-associated organic carbon (MAOC) and SOC, across depths in the study area grasslands (a, b) and global grasslands (c, d), with depth as a random effect. The inset figures display the fixed and random coefficients of the effects. R^2 indicates the total variance explained by the fixed and random effects. Data presented in (a, b) are sampled and measured in the study area, while those in (c, d) are from global temperate grasslands derived from Georgiou et al. (2022).

total variance in POC, MAOC, and MAOC:(MAOC+POC) (Figure 4). The first two canonical axes, RDA1 and RDA2, contributed 39.43% and 18.35%, respectively, to the explained variance. Regarding individual SOC components, POC was closely positively associated with MAP (the angle of the arrows representing POC and MAP was close to 0°) but negatively associated with soil pH and depth (the angle of the arrows was close to 180°), whereas MAOC was closely positively associated with Al but negatively associated with altitude (Figure 4). MAOC:(MAOC+POC) had the strongest positive association with CS but was negatively associated with GI and thermal_c34 (Figure 4). Furthermore, HP quantified the relative importance of each factor (Table S4). The results identified CS, Al, soil pH, MAP, and soil depth as the five most dominant variables determining the partitioning of SOC components, with respective relative contributions of 26.27%, 17.72%, 17.36%, 10.09%, and 8.90% (Table S4).

Path modeling further identified the direct and indirect effects of the key driving factors identified by RDA, which explained 57%, 67%, and 56% of the variance in POC, MAOC, and MAOC:(MAOC+POC), respectively (Figure 5). For POC, all five latent variables except terrain had significant direct effects (p<0.05), with edaphic attributes indicated by Al, pH, and CS exhibiting the strongest direct effects (path coefficient ρ=0.40), followed by soil depth (ρ=−0.37), climate (ρ=0.22), and human disturbance (ρ=0.20). For MAOC, edaphic attributes also had the strongest direct effect (ρ=0.58), followed by climate (ρ=0.29) and soil depth (ρ=−0.22), and only the influences of these three variables were significant (p<0.05). Regarding MAOC:(MAOC+POC), only edaphic attributes (ρ=0.56), soil depth (ρ=0.23), and human disturbance (ρ=−0.29) had significant and direct influences among all variables. Additionally, climate and human disturbance indirectly influenced the three carbon variables through their effects on edaphic attributes (Figure 5).

To further investigate the impacts of the four most important factors (CS, Al, pH, and MAP) identified by RDA on POC, MAOC, and MAOC:(MAOC+POC) along the soil profile, BLMMs were fitted with these factors as fixed effects and soil depth as a random effect (Figure 6). In particular, the influence of MAP on POC weakened with increasing soil depth, and the coefficients of the effects decreased from 0.96 (0.45–1.45, with the 95% credible interval) in the 0–10 cm layer to 0.02 (−0.23–0.26) in the 150–200 cm layer. Additionally, CS content showed a significant positive effect on POC accumulation only in the 0–20 cm layer, while soil pH exhibited a significant negative effect in the 0–50 cm layer. In contrast, Al had no significant influence on POC across all soil layers. For MAOC, the driving mechanism was distinctly different from that of POC, being almost entirely dominated by soil properties. For

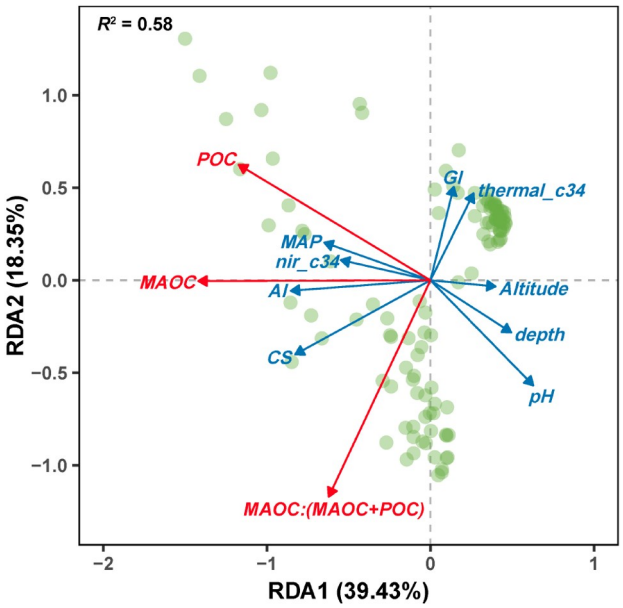

Figure 4 Redundancy analysis revealing relationships of particulate organic carbon (POC), mineral-associated organic carbon (MAOC), and the proportion of MAOC to total soil organic carbon (MAOC:(MAOC+POC)) with various variables in the grasslands of the study area. The first and second RDA axes account for 39.43% and 18.35% of the variance in the soil carbon fraction metrics, respectively. For the top five variables contributing to the SOC components, the order from highest to lowest is CS, Al, pH, MAP, and depth, with contribution rates of 26.27%, 17.72%, 17.36%, 10.09%, and 8.90%, respectively. Refer to Table S4 for explanations of the abbreviations.

example, the effects of both Al and CS on MAOC were generally stronger in the 0–30 cm layer. However, only Al maintained a significant effect on MAOC in the 30–100 cm layer. In comparison, soil pH exerted only a weak negative effect throughout the profile, while MAP had almost no influence. For MAOC:(MAOC+POC), the direction of the influence of the assessed variables did not change but varied across depths. Notably, among all factors, only CS demonstrated a significant and relatively stable positive influence across all soil layers, with coefficients of the effects ranging from 0.67 (0.23–0.99) to 0.82 (0.47–1.29).

4. Discussion

4.1 Depth distribution of SOC, POC, and MAOC

Our results indicate that both POC and MAOC contents in the Inner Mongolian grasslands decreased rapidly with increasing soil depth (Figure 2), which largely mirrored the decreasing inputs of exogenous organic matter with depth associated with root biomass. Indeed, Ma et al. (2008) reported that in the Inner Mongolian grasslands, 47% of the root biomass is concentrated in the top 0–10 cm of soil, suggesting that deep soil layers receive less carbon from roots. In addition to plant residue inputs, dissolved organic

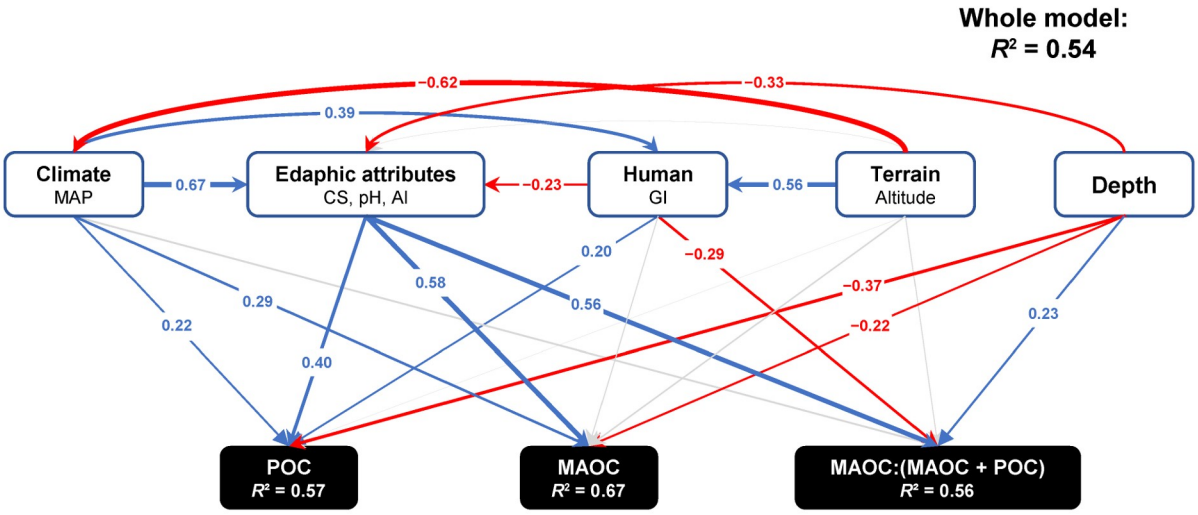

Figure 5 Schematic representation of the path analyses used to identify the controls on soil particulate organic carbon (POC), mineral-associated organic carbon (MAOC), and the proportion of MAOC to total soil organic carbon (MAOC:(MAOC+POC)) in the grasslands of the study area. The arrows indicate the direction of the effects, whereas the blue and red paths represent positive and negative effects, respectively. The numbers and the line width both represent path coefficients obtained from path analysis, indicating the direct and indirect effects of the variables. The relevant latent variables are the same as those in Figure 4. The R^2 value within the box represents the coefficient of determination for the corresponding variable (i.e., POC, MAOC, and MAOC:(MAOC+POC)), whereas that outside the circular panel represents the coefficient of determination for the whole path model.

matter (DOM) represents a significant source of both POC and MAOC (Dubeux Jr et al., 2024; Si et al., 2024). However, the arid and semiarid conditions in the Inner Mongolian grasslands, which are characterized by low precipitation and high evapotranspiration, likely constrain the downward movement of DOM and its contribution to carbon accumulation in deep soil layers (Begill et al., 2023; Zhou et al., 2023).

MAOC to total SOC ratio typically increased with depth due to enhanced physical protection in deeper soil layers and the accumulation of finer carbon components transported downward from the topsoil (Sokol et al., 2019; Lavallee et al., 2020; Hicks Pries et al., 2023). However, our results revealed nonlinear changes in the MAOC to total SOC ratio in the Inner Mongolian grasslands. In the 0–50 cm soil layer, as expected, the ratio increased with depth, which is consistent with observations from Australian temperate grasslands in similar depth ranges of 0–30 cm (Román Dobarco et al., 2023). This increase in the fraction of MAOC in total SOC could be attributed to the increasing contribution of microbial necromass to total SOC with depth, as demonstrated by several studies (Ma et al., 2018; Wang B R et al., 2021; Sokol et al., 2022; Liang et al., 2024). More interestingly, we found that the proportion of MAOC to total SOC consistently decreased with depth in the 50–200 cm layer. Initially, we considered the possibility of carbon saturation in deep layers, hypothesizing that the mineral surfaces may have reached their upper capacity for carbon adsorption (Six et al., 2002; Stewart et al., 2007). However, fitting a suite of models (including linear, logarithmic, saturation, S-curve, and inverse models) to describe the MAOC-SOC relationships, we found that the linear model consistently outperformed all nonlinear alternatives across all depth layers (Table S5). This pattern suggests that carbon accumulation in MAOC remains proportional to SOC, and that mineral surfaces in our study region have not yet reached saturation thresholds. We therefore propose that the declining MAOC:SOC ratio in deeper layers reflects increasing environmental constraints on microbial activity rather than mineral saturation. Specifically, subsoil microbes face strong limitations in acquiring high-quality substrates for energy and nutrient assimilation (Fontaine et al., 2007), compounded by reduced oxygen availability (Rumpel and Kögel-Knabner, 2011). These constraints can inhibit microbial growth and metabolism (Bernal et al., 2016), thereby limiting the production of microbial necromass—a major precursor of MAOC formation (Liang et al., 2019). Additionally, POC decomposition may be much slower in deeper soil layers, promoting its accumulation and thus diluting the fraction of MAOC in total SOC. Taken together, these results suggest that physiological and resource-based constraints on microbial processing, rather than mineral saturation, are key bottlenecks for MAOC accumulation in deep soil layers. These findings highlight the importance of considering deeper soil layers in carbon sequestration, as they may have a significant impact on the long-term stability of soil carbon pools. For example, practices like optimizing plant community composition to include deeper-rooted perennial grasses, diversifying species to enhance root system complementarity, and improving grazing management have been recommended to effectively enhance carbon accumulation in deep layers (Li et al., 2019; Luo et al., 2024).

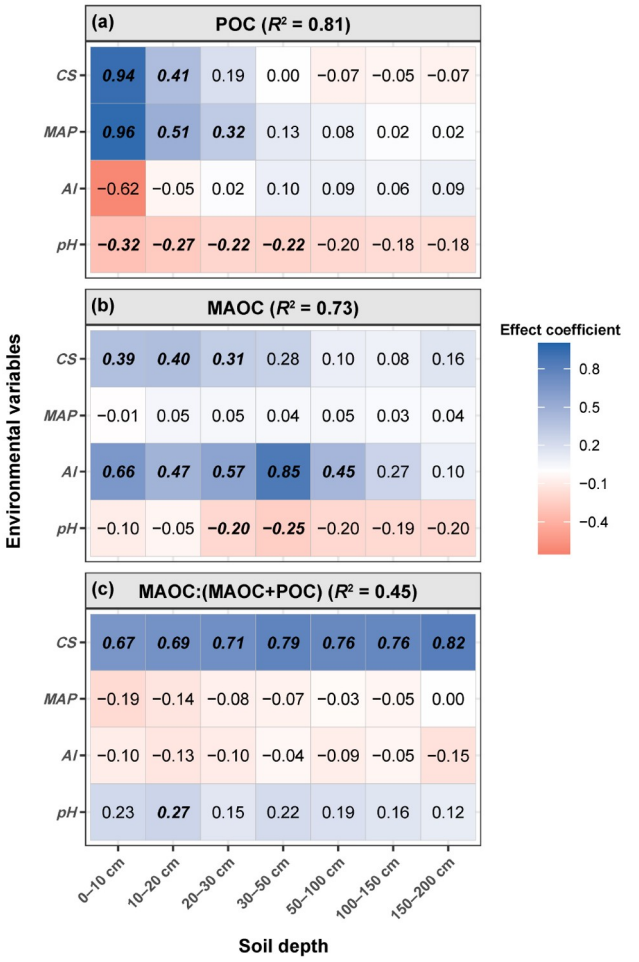

Figure 6 Bayesian linear mixed-effects modeling of relationships between particulate organic carbon (POC) (a), mineral-associated organic carbon (MAOC) (b), and the proportion of MAOC to total soil organic carbon (MAOC:(MAOC+POC)) (c), and the most important drivers derived by redundancy analysis in the grasslands of the study area. The color grids show the coefficients of linear mixed-effects regression models for POC, MAOC, and MAOC:(MAOC+POC), with depth treated as a random effect. Bold italic values indicate significant relationships (95% credible interval does not include zero).

While numerous studies have reported a dominance of MAOC in global grassland soils, exceeding 60% of total SOC, particularly in surface soils (Cotrufo et al., 2019; Bai and Cotrufo, 2022; Hansen et al., 2023), our findings from the Inner Mongolian grasslands present a contrasting pattern, where POC dominates over MAOC. This discrepancy may be attributed to the post-degradation recovery phase of these grasslands. During grassland restoration, vegetation productivity typically recovers faster than soil physicochemical properties, particularly those related to texture and mineralogy. For instance, Liao et al. (2023) found that POC is more sensitive to vegetation recovery during grassland restoration in the Loess Plateau. This faster accumulation of plant-derived carbon inputs likely contributes to the relatively high POC:SOC ratio observed in our study region. In contrast, the formation and stabilization of MAOC are strongly influenced by soil texture, particularly the abundance of fine particles (i.e., clay and silt content), which enhances microbial habitat quality, water retention, and the potential for organo-mineral associations (Mao et al., 2024). However, historical overgrazing and degradation across Inner Mongolia have led to widespread soil coarsening, with losses of clay and silt content and increases in sand content—a process often associated with desertification (Zhang et al., 2020; Zheng et al., 2024b). Consistent with this, our study area exhibits a coarser soil texture (Table S6), with an average clay and silt content of 28%, compared to 56% in global grasslands (Hansen et al., 2023). The recovery of fine mineral fractions is a slow and long-term process, typically requiring several decades or more (Liu M et al., 2025). Therefore, despite increasing carbon inputs from recovering vegetation, the limited mineral surface area and physical protection associated with coarser soils likely constrain the microbial transformation of POC into MAOC and reduce MAOC stability (Mao et al., 2024). Together, these findings suggest that the current dominance of labile POC over stable MAOC in the Inner Mongolian grasslands would reflect an early stage of ecosystem recovery, in which carbon inputs are increasing, but stabilization mechanisms remain underdeveloped. This implies a higher vulnerability of SOC to disturbance or loss, and highlights the need for continued ecological restoration and sustainable land management practices to enhance long-term carbon stabilization through both biotic and abiotic pathways.

4.2 Depth-dependent influence of environmental factors on SOC fractions

Our study revealed depth-dependent controls on SOC fractions (Figure 6). Topsoil POC is regulated primarily by the balance between plant litter inputs and microbial decomposition. A higher MAP generally leads to greater plant productivity, especially in water-limited ecosystems, contributing to increased litter inputs and, consequently, higher POC contents (Wiesmeier et al., 2019). This finding aligns with the study by Díaz-Martínez et al. (2024), who reported a positive correlation between precipitation and topsoil POC in global drylands. Similarly, clay and silt, with their relatively high water-holding capacities, create favorable environments for plant growth and microbial activity, indirectly contributing to POC accumulation (Mao et al., 2024), as evidenced by the positive correlation between CS and POC (Figure 6). However, this correlation becomes insignificant in deeper layers. One potential explanation is that in deeper soil layers, POC derived from plant roots and root exudates is relatively limited, and most POC in these deeper layers may originate from downward transport from upper soil layers, thereby attenuating the direct influence of CS on POC ac-

cumulation (Rumpel and Kögel-Knabner, 2011). Soil pH generally negatively affects POC across the entire soil profile. A lower pH has been reported to influence microbial community composition and activity, leading to slower POC decomposition, especially at cooler temperatures (Nedwell, 1999; Rousk et al., 2009). As most root-derived carbon inputs are concentrated in surface soils (Wang et al., 2023), the impacts of climatic and edaphic attributes on POC decrease with increasing soil depth (Figure 6).

The factors influencing MAOC varied with soil depth, with MAOC being coregulated by CS and Al oxide in surface layers but predominantly controlled by Al oxide at intermediate depths (Figure 6). This vertical shift in dominant controlling mechanisms can be attributed to the changing nature and availability of organic matter, as well as the varying importance of different stabilization processes across soil layers. In topsoil, the abundant input of fresh, partially decomposed organic matter leads to complex interactions between organic compounds and various soil minerals. Clay and silt particles play crucial roles in this context, as their large specific surface area facilitates the adsorption and occlusion of organic matter into stable aggregates (Kleber et al., 2015). In addition, the binding of organic compounds with metal ions, oxides, and minerals, such as Al, also contributes to the stabilization of MAOC in surface layers (Rowley et al., 2018; Kang et al., 2024). However, as soil depth increases, the supply of fresh organic matter decreases, and biological activity becomes more limited. This results in slower decomposition rates of organic matter in deeper layers. Under these conditions, the higher surface area-to-volume ratio and greater number of bonding sites of Al oxide make them the dominant mineral phase controlling MAOC stabilization compared with the other phases, overshadowing the role of clay minerals (Lalonde et al., 2012). In addition, MAOC:(MAOC+POC), an indicator of SOC stability, was significantly correlated with CS across the entire soil profile, with its correlation strengthening with depth. This finding highlights the growing importance of physical protection mechanisms in deeper soil layers where biological decomposition is limited in the Inner Mongolian grasslands (Henneron et al., 2022; Hicks Pries et al., 2023).

4.3 Implications for SOC sequestration in the Inner Mongolian grasslands

On the basis of the findings of this study, we propose two strategies for SOC sequestration in Inner Mongolian or similar grasslands, focusing on short-term and long-term carbon sequestration, respectively. In the short term, increasing topsoil POC should be prioritized. Compared with MAOC, POC has a faster accumulation rate and greater sensitivity to management practices (Liao et al., 2023). Given the plant litter-derived origin of POC, strategies aimed at increasing plant carbon input, such as re-establishing native vegetation (Török et al., 2021) and increasing plant diversity (Lange et al., 2015), are particularly effective, especially in water-limited regions. While greater carbon inputs may also stimulate priming effects that enhance microbial decomposition of existing SOC, emerging evidence suggests that the net direction of SOC change following vegetation restoration depends on the initial soil carbon content (Hong et al., 2020). Specifically, in low-carbon soils such as those found in degraded Inner Mongolian grasslands, vegetation restoration is highly likely to result in net carbon gains (Hong et al., 2020). Furthermore, our recent study (Zheng et al., 2024b) underscores the significant role of ecological protection measures in areas with low rainfall and severe degradation, where these strategies can yield substantial benefits for SOC sequestration. Hence, priority regions for enhancing plant growth and POC sequestration might often coincide with areas where limiting factors, such as water availability, nutrient status, soil health, and climate resilience, can be effectively addressed through targeted management practices.

While increasing POC is a crucial step for short-term carbon sequestration, its inherent instability necessitates a focus on long-term stabilization. To ensure sustained carbon storage, promoting the sequestration of MAOC is essential. MAOC, which is relatively resistant to decomposition, can potentially contribute to long-term soil carbon sequestration. Therefore, a comprehensive approach that combines strategies to increase POC inputs and promote MAOC formation is necessary for effective carbon management in grassland ecosystems (Poeplau et al., 2018). While CS and Al oxide play significant roles in stabilizing MAOC, directly altering their abundance in vast natural grasslands such as Inner Mongolia is impractical because of their geological origins and long-term weathering processes. However, we can indirectly influence soil properties and the organic matter content to increase carbon sequestration. The implementation of sustainable grazing practices, such as rotational grazing and rest periods, can reduce soil degradation and promote plant growth (Bai and Cotrufo, 2022). Nutrient management strategies, including balanced fertilization and manure application, can optimize plant growth and carbon uptake. Additionally, adopting climate-resilient grass species and efficient irrigation systems can mitigate climate change impacts and increase long-term carbon storage. By integrating these strategies, we can maximize the potential of grassland ecosystems to sequester both POC and MAOC.

5. Conclusion

This study provides a detailed analysis of the vertical distribution and controlling factors of SOC fractions in the Inner Mongolian grasslands, based on soil profile measurements

extending to a depth of 2 m. The results revealed that POC generally dominated over MAOC across all soil layers. The driving mechanisms of climate and soil attributes varied for different components and depths of SOC. In the topsoil (0–0.3 m), POC was primarily regulated by climate variables (e.g., mean annual precipitation) and soil properties (e.g., clay and silt content and soil pH). These influences on POC generally diminished in deeper soil layers. In contrast, MAOC at all depths was mainly governed by soil properties (e.g., clay and silt content and Al oxide), with climatic factors showing no significant impact. These findings underscore the importance of depth-specific strategies for SOC sequestration, emphasizing the enhancement of POC for rapid SOC accumulation and stabilization of MAOC for long-term carbon storage.

Acknowledgements *This work was supported by the National Natural Science Foundation of China (Grant Nos. 42375116 & 32241036).*

Conflict of interest The authors declare no conflict of interest.

Supporting information The supporting information is available online at http://earth.scichina.com and http://link.springer.com. The supporting materials are published as submitted, without typesetting or editing. The responsibility for scientific accuracy and content remains entirely with the authors.

References

Akinwande M O, Dikko H G, Samson A. 2015. Variance inflation factor: As a condition for the inclusion of suppressor variable(s) in regression analysis. Open J Stat, 05: 754–767

Amatulli G, Domisch S, Tuanmu M N, Parmentier B, Ranipeta A, Malczyk J, Jetz W. 2018. A suite of global, cross-scale topographic variables for environmental and biodiversity modeling. Sci Data, 5: 1–5

Bai Y F, Cotrufo M F. 2022. Grassland soil carbon sequestration: Current understanding, challenges, and solutions. Science, 377: 603–608

Begill N, Don A, Poeplau C. 2023. No detectable upper limit of mineral-associated organic carbon in temperate agricultural soils. Glob Change Biol, 29: 4662–4669

Bernal B, McKinley D C, Hungate B A, White P M, Mozdzer T J, Megonigal J P. 2016. Limits to soil carbon stability; Deep, ancient soil carbon decomposition stimulated by new labile organic inputs. Soil Biol Biochem, 98: 85–94

Briedis C, Sá J C M, Caires E F, Navarro J F, Inagaki T M, Boer A, Neto C Q, Ferreira A O, Canalli L B, Santos J B. 2012. Soil organic matter pools and carbon-protection mechanisms in aggregate classes influenced by surface liming in a no-till system. Geoderma, 170: 80–88

Button E S, Pett-Ridge J, Murphy D V, Kuzyakov Y, Chadwick D R, Jones D L. 2022. Deep-C storage: Biological, chemical and physical strategies to enhance carbon stocks in agricultural subsoils. Soil Biol Biochem, 170: 108697

Ciesielski H, Sterckeman T, Santerne M, Willery J P. 1997. A comparison between three methods for the determination of cation exchange capacity and exchangeable cations in soils. Agronomie, 17: 9–16

Collignon C, Ranger J, Turpault M P. 2012. Seasonal dynamics of Al- and Fe-bearing secondary minerals in an acid forest soil: Influence of Norway spruce roots (*Picea abies* (L.) Karst.). Eur J Soil Sci, 63: 592–602

Cotrufo M F, Ranalli M G, Haddix M L, Six J, Lugato E. 2019. Soil carbon storage informed by particulate and mineral-associated organic matter. Nat Geosci, 12: 989–994

Díaz-Martínez P, Maestre F T, Moreno-Jiménez E, Delgado-Baquerizo M, Eldridge D J, Saiz H, Gross N, Le Bagousse-Pinguet Y, Gozalo B, Ochoa V, Guirado E, García-Gómez M, Valencia E, Asensio S, Berdugo M, Martínez-Valderrama J, Mendoza B J, García-Gil J C, Zaccone C, Panettieri M, García-Palacios P, Fan W, Benavente-Ferraces I, Rey A, Eisenhauer N, Cesarz S, Abedi M, Ahumada R J, Alcántara J M, Amghar F, Aramayo V, Arroyo A I, Bahalkeh K, Ben Salem F, Blaum N, Boldgiv B, Bowker M A, Bran D, Branquinho C, Bu C F, Cáceres Y, Canessa R, Castillo-Monroy A P, Castro I, Castro-Quezada P, Chibani R, Conceição A A, Currier C M, Darrouzet-Nardi A, Deák B, Dickman C R, Donoso D A, Dougill A J, Durán J, Ejtehadi H, Espinosa C, Fajardo A, Farzam M, Ferrante D, Fraser L H, Gaitán J J, Gusman Montalván E, Hernández-Hernández R M, von Hessberg A, Hölzel N, Huber-Sannwald E, Hughes F M, Jadán-Maza O, Geissler K, Jentsch A, Ju M C, Kaseke K F, Kindermann L, Koopman J E, Le Roux P C, Liancourt P, Linstädter A, Liu J S, Louw M A, Maggs-Kölling G, Makhalanyane T P, Issa O M, Marais E, Margerie P, Mazaneda A J, McClaran M P, Messeder J V S, Mora J P, Moreno G, Munson S M, Nunes A, Oliva G, Oñatibia G R, Osborne B, Peter G, Pueyo Y, Quiroga R E, Reed S C, Reyes V M, Rodríguez A, Ruppert J C, Sala O, Salah A, Sebei J, Sloan M, Solongo S, Stavi I, Stephens C R A, Teixido A L, Thomas A D, Throop H L, Tielbörger K, Travers S, Val J, Valko O, van den Brink L, Velbert F, Wamiti W, Wang D L, Wang L X, Wardle G M, Yahdjian L, Zaady E, Zeberio J M, Zhang Y M, Zhou X B, Plaza C. 2024. Vulnerability of mineral-associated soil organic carbon to climate across global drylands. Nat Clim Chang, 14: 976–982

Dondini M, Martin M, De Camillis C, Uwizeye A, Soussana J F, Robinson T, Steinfeld H. 2023. Global assessment of soil carbon in grasslands—From current stock estimates to sequestration potential. Rome: FAO. 76

Dubeux Jr J C B, Lira Junior M A, Simili F F, Bretas I L, Trumpp K R, Bizzuti B E, Garcia L, Oduor K T, Queiroz L M D, Acuña J P, Mendes C T E. 2024. Deep soil organic carbon: A review. CABI Rev, cabireviews.2024.0024

Estop-Aragonés C, Olefeldt D, Abbott B W, Chanton J P, Czimczik C I, Dean J F, Egan J E, Gandois L, Garnett M H, Hartley I P, Hoyt A, Lupascu M, Natali S M, O'Donnell J A, Raymond P A, Tanentzap A J, Tank S E, Schuur E A G, Turetsky M, Anthony K W. 2020. Assessing the potential for mobilization of old soil carbon after permafrost thaw: A synthesis of ^{14}C measurements from the northern permafrost region. Glob Biogeochem Cycle, 34: e2020GB006672

Fick S E, Hijmans R J. 2017. WorldClim 2: New 1-km spatial resolution climate surfaces for global land areas. Intl J Climatol, 37: 4302–4315

Fontaine S, Barot S, Barré P, Bdioui N, Mary B, Rumpel C. 2007. Stability of organic carbon in deep soil layers controlled by fresh carbon supply. Nature, 450: 277–280

Georgiou K, Jackson R B, Vindušková O, Abramoff R Z, Ahlström A, Feng W T, Harden J W, Pellegrini A F A, Polley H W, Soong J L, Riley W J, Torn M S. 2022. Global stocks and capacity of mineral-associated soil organic carbon. Nat Commun, 13: 3797

Gilbert M, Nicolas G, Cinardi G, Van Boeckel T P, Vanwambeke S O, Wint G R W, Robinson T P. 2018. Global distribution data for cattle, buffaloes, horses, sheep, goats, pigs, chickens and ducks in 2010. Sci Data, 5: 1

González C M, Orellana L C, Casanovas S S, Pignata M L. 1998. Environmental conditions and chemical response of a transplanted lichen to an urban area. J Environ Manage, 53: 73–81

Hansen P M, Even R, King A E, Lavallee J, Schipanski M, Cotrufo M F. 2023. Distinct, direct and climate-mediated environmental controls on global particulate and mineral-associated organic carbon storage. Glob Change Biol, 30: e17080

Harris D, Horwáth W R, van Kessel C. 2001. Acid fumigation of soils to remove carbonates prior to total organic carbon or CARBON-13 isotopic analysis. Soil Sci Soc Amer J, 65: 1853–1856

Henneron L, Balesdent J, Alvarez G, Barré P, Baudin F, Basile-Doelsch I, Cécillon L, Fernandez-Martinez A, Hatté C, Fontaine S. 2022. Bioe-

nergetic control of soil carbon dynamics across depth. Nat Commun, 13: 7676
Hicks Pries C E, Castanha C, Porras R C, Torn M S. 2017. The whole-soil carbon flux in response to warming. Science, 355: 1420–1423
Hicks Pries C E, Ryals R, Zhu B, Min K, Cooper A, Goldsmith S, Pett-Ridge J, Torn M, Berhe A A. 2023. The deep soil organic carbon response to global change. Annu Rev Ecol Evol Syst, 54: 375–401
Hong S B, Yin G D, Piao S L, Dybzinski R, Cong N, Li X Y, Wang K, Peñuelas J, Zeng H, Chen A P. 2020. Divergent responses of soil organic carbon to afforestation. Nat Sustain, 3: 694–700
Jobbágy E G, Jackson R B. 2000. The vertical distribution of soil organic carbon and its relation to climate and vegetation. Ecol Appl, 10: 423
Kang J, Qu C C, Chen W L, Cai P, Chen C R, Huang Q Y. 2024. Organo-organic interactions dominantly drive soil organic carbon accrual. Glob Change Biol, 30: e17147
Kleber M, Eusterhues K, Keiluweit M, Mikutta C, Mikutta R, Nico P S. 2015. Mineral-organic associations: Formation, properties, and relevance in soil environments. Adv Agron, 130: 1–140
Lai J S, Zou Y, Zhang J L, Peres-Neto P R. 2022. Generalizing hierarchical and variation partitioning in multiple regression and canonical analyses using the rdacca.hp R package. Methods Ecol Evol, 13: 782–788
Lalonde K, Mucci A, Ouellet A, Gélinas Y. 2012. Preservation of organic matter in sediments promoted by iron. Nature, 483: 198–200
Lange M, Eisenhauer N, Sierra C A, Bessler H, Engels C, Griffiths R I, Mellado-Vázquez P G, Malik A A, Roy J, Scheu S, Steinbeiss S, Thomson B C, Trumbore S E, Gleixner G. 2015. Plant diversity increases soil microbial activity and soil carbon storage. Nat Commun, 6: 6707
Lavallee J M, Soong J L, Cotrufo M F. 2020. Conceptualizing soil organic matter into particulate and mineral-associated forms to address global change in the 21st century. Glob Change Biol, 26: 261–273
Legendre P, Legendre L. 1988. Numerical Ecology. 2nd ed. Amsterdam: Elsevier. 853
Li J P, Ma H B, Xie Y Z, Wang K B, Qiu K Y. 2019. Deep soil C and N pools in long-term fenced and overgrazed temperate grasslands in northwest China. Sci Rep, 9: 16088
Liang C, Schimel J P, Jastrow J D. 2017. The importance of anabolism in microbial control over soil carbon storage. Nat Microbiol, 2: 1–6
Liang C, Amelung W, Lehmann J, Kästner M. 2019. Quantitative assessment of microbial necromass contribution to soil organic matter. Glob Change Biol, 25: 3578–3590
Liang Y T, Hu H, Crowther T W, Jörgensen R G, Liang C, Chen J, Sun Y S, Liu C Y, Ding J X, Huang A D, Zhou J H, Zhang J B. 2024. Global decline in microbial-derived carbon stocks with climate warming and its future projections. Natl Sci Rev, 11: nwae330
Liao J J, Yang X, Dou Y X, Wang B R, Xue Z J, Sun H, Yang Y, An S S. 2023. Divergent contribution of particulate and mineral-associated organic matter to soil carbon in grassland. J Environ Manage, 344: 118536
Liu L L, Sayer E J, Deng M F, Li P, Liu W X, Wang X, Yang S, Huang J S, Luo J, Su Y J, Grünzweig J M, Jiang L, Hu S J, Piao S L. 2023. The grassland carbon cycle: Mechanisms, responses to global changes, and potential contribution to carbon neutrality. Fundamental Res, 3: 209–218
Liu M, Liu S B, Xu X L, Soromotin A V, Kuzyakov Y. 2025. Does restoration of degraded grasslands follow the theory of multiple stable states? Agr Ecosyst Environ, 383: 109508
Liu M L, Zheng S L, Pendall E, Smith P, Liu J J, Li J Q, Fang C M, Li B, Nie M. 2025. Unprotected carbon dominates decadal soil carbon increase. Nat Commun, 16: 2008
Luo Z K, Viscarra Rossel R A, Shi Z. 2020. Distinct controls over the temporal dynamics of soil carbon fractions after land use change. Glob Change Biol, 26: 4614–4625
Luo Z K, Zhang S, Zhao Z G, Minasny B, Chang J F, Huang J Y, Li B H, Shi Z, Wang E L, Wang M M, Wu Y S, Xiao L J, Ye S. 2024. Soil-smart cropping for climate-smart production. Geoderma, 451: 117061
Ma T, Zhu S S, Wang Z H, Chen D M, Dai G H, Feng B W, Su X Y, Hu H F, Li K H, Han W X, Liang C, Bai Y F, Feng X J. 2018. Divergent accumulation of microbial necromass and plant lignin components in grassland soils. Nat Commun, 9: 3480
Ma W H, Yang Y H, He J S, Zeng H, Fang J Y. 2008. Above- and belowground biomass in relation to environmental factors in temperate grasslands, Inner Mongolia. Sci China Ser C-Life Sci, 51: 263–270
Mao H R, Cotrufo M F, Hart S C, Sullivan B W, Zhu X F, Zhang J C, Liang C, Zhu M Q. 2024. Dual role of silt and clay in the formation and accrual of stabilized soil organic carbon. Soil Biol Biochem, 192: 109390
Minasny B, McBratney A B. 2001. The Australian soil texture boomerang: A comparison of the Australian and USDA/FAO soil particle-size classification systems. Soil Res, 39: 1443–1451
Nedwell D B. 1999. Effect of low temperature on microbial growth: Lowered affinity for substrates limits growth at low temperature. FEMS Microbiol Ecol, 30: 101–111
Poeplau C, Don A, Six J, Kaiser M, Benbi D, Chenu C, Cotrufo M F, Derrien D, Gioacchini P, Grand S, Gregorich E, Griepentrog M, Gunina A, Haddix M, Kuzyakov Y, Kühnel A, Macdonald L M, Soong J, Trigalet S, Vermeire M L, Rovira P, van Wesemael B, Wiesmeier M, Yeasmin S, Yevdokimov I, Nieder R. 2018. Isolating organic carbon fractions with varying turnover rates in temperate agricultural soils—A comprehensive method comparison. Soil Biol Biochem, 125: 10–26
R Core Team. 2024. R: A Language and Environment for Statistical Computing. Vienna: The R Foundation for Statistical Computing
Rocci K S, Lavallee J M, Stewart C E, Cotrufo M F. 2021. Soil organic carbon response to global environmental change depends on its distribution between mineral-associated and particulate organic matter: A meta-analysis. Sci Total Environ, 793: 148569
Román Dobarco M, Wadoux A M J C, Malone B, Minasny B, McBratney A B, Searle R. 2023. Mapping soil organic carbon fractions for Australia, their stocks, and uncertainty. Biogeosciences, 20: 1559–1586
Rousk J, Brookes P C, Baath E. 2009. Contrasting soil pH effects on fungal and bacterial growth suggest functional redundancy in carbon mineralization. Appl Environ Microbiol, 75: 1589–1596
Rowley M C, Grand S, Verrecchia É P. 2018. Calcium-mediated stabilisation of soil organic carbon. Biogeochemistry, 137: 27–49
Rumpel C, Kögel-Knabner I. 2011. Deep soil organic matter—A key but poorly understood component of terrestrial C cycle. Plant Soil, 338: 143–158
Schiedung M, Don A, Beare M H, Abiven S. 2023. Soil carbon losses due to priming moderated by adaptation and legacy effects. Nat Geosci, 16: 909–914
Si Q T N, Chen K L, Wei B, Zhang Y W, Sun X, Liang J Y. 2024. Dissolved carbon flow to particulate organic carbon enhances soil carbon sequestration. Soil, 10: 441–450
Six J, Guggenberger G, Paustian K, Haumaier L, Elliott E T, Zech W. 2001. Sources and composition of soil organic matter fractions between and within soil aggregates. Eur J Soil Sci, 52: 607–618
Six J, Conant R T, Paul E A, Paustian K. 2002. Stabilization mechanisms of soil organic matter: Implications for C-saturation of soils. Plant Soil, 241: 155–176
Sokol N W, Sanderman J, Bradford M A. 2019. Pathways of mineral-associated soil organic matter formation: Integrating the role of plant carbon source, chemistry, and point of entry. Glob Change Biol, 25: 12–24
Sokol N W, Whalen E D, Jilling A, Kallenbach C, Pett-Ridge J, Georgiou K. 2022. Global distribution, formation and fate of mineral-associated soil organic matter under a changing climate: A trait-based perspective. Funct Ecol, 36: 1411–1429
Stewart C E, Paustian K, Conant R T, Plante A F, Six J. 2007. Soil carbon saturation: Concept, evidence and evaluation. Biogeochemistry, 86: 19–31
Sun S Y, Liu X F, Lu S X, Cao P L, Hui D F, Chen J, Guo J F, Yang Y S. 2023. Depth-dependent response of particulate and mineral-associated organic carbon to long-term throughfall reduction in a subtropical natural forest. Catena, 223: 106904

Tang K Z, Wu C, Wang S, Liao W J, Yin L C, Zhou W J, Cui H J. 2024. Distribution characteristics of soil organic carbon fractions in paddy profiles with 40 years of fertilization under two groundwater levels. J Soils Sediments, 24: 681–691

Ter Braak C J F, Prentice I C. 1988. A theory of gradient analysis. In: Begon M, Fitter A H, Ford E D, Macfadyen A, eds. Advances in Ecological Research. London: Academic Press. 271–317

Török P, Brudvig L A, Kollmann J, N. Price J, Tóthmérész B. 2021. The present and future of grassland restoration. Restoration Ecol, 29: e13378

Wagner H H. 2004. Direct multi-scale ordination with canonical correspondence analysis. Ecology, 85: 342–351

Wang B R, An S S, Liang C, Liu Y, Kuzyakov Y. 2021. Microbial necromass as the source of soil organic carbon in global ecosystems. Soil Biol Biochem, 162: 108422

Wang G C, Luo Z K, Huang Y, Sun W J, Wei Y R, Xiao L J, Deng X, Zhu J H, Li T T, Zhang W. 2021. Simulating the spatiotemporal variations in aboveground biomass in Inner Mongolian grasslands under environmental changes. Atmos Chem Phys, 21: 3059–3071

Wang G C, Luo Z K, Huang Y, Xia X A, Wei Y R, Lin X H, Sun W J. 2022a. Preseason heat requirement and days of precipitation jointly regulate plant phenological variations in Inner Mongolian grassland. Agric For Meteor, 314: 108783

Wang G C, Xiao M J, Xia X A, Huang Y, Luo Z K, Wei Y R, Zhang W. 2022b. Chilling accumulation is not an effective predictor of vegetation green-up date in inner mongolian grasslands. Geophys Res Lett, 49: e2021GL096558

Wang G C, Xiao L J, Lin Z Q, Zhang Q, Guo X W, Cowie A, Zhang S, Wang M M, Chen S C, Zhang G L, Shi Z, Sun W J, Luo Z K. 2023. Most root-derived carbon inputs do not contribute to long-term global soil carbon storage. Sci China Earth Sci, 66: 1072–1086

Wiesmeier M, Urbanski L, Hobley E, Lang B, von Lützow M, Marin-Spiotta E, van Wesemael B, Rabot E, Ließ M, Garcia-Franco N, Wollschläger U, Vogel H J, Kögel-Knabner I. 2019. Soil organic carbon storage as a key function of soils—A review of drivers and indicators at various scales. Geoderma, 333: 149–162

Zhang Q, Buyantuev A, Fang X N, Han P, Li A, Li F Y, Liang C Z, Liu Q F, Ma Q, Niu J M, Shang C W, Yan Y Z, Zhang J. 2020. Ecology and sustainability of the Inner Mongolian Grassland: Looking back and moving forward. Landsc Ecol, 35: 2413–2432

Zhao M S, Heinsch F A, Nemani R R, Running S W. 2005. Improvements of the MODIS terrestrial gross and net primary production global data set. Remote Sens Environ, 95: 164–176

Zheng H J, Yang X F, Song C Q, Zhang W, Sun W J, Wang G C. 2024a. Distinct environmental controls on above- and below-ground net primary productivity in Northern China's grasslands. Ecol Indicators, 167: 112717

Zheng H J, Huang Y, Zhang W, Song C Q, Zhang Q, Sun W J, Yu Y Q, Yu L J, Li H G, Zhang C H, Jiang W F, Yang X Y, Wang G C. 2024b. The implementation of ecological protection in Inner Mongolia has slowed down grassland degradation. Fundamental Res, http://doi.org/10.1016/j.fmre.2024.10.006

Zhou H, Gan F L, Dai Q H, Yan Y J, Xu X J, Zhang Y, Hu Z Y, Zhao M. 2023. Migration of dissolved carbon on bare karst slopes in soil in response to natural rainfall events. Geoderma, 436: 116527

Zhou Z H, Ren C J, Wang C K, Delgado-Baquerizo M, Luo Y Q, Luo Z K, Du Z G, Zhu B, Yang Y H, Jiao S, Zhao F Z, Cai A D, Yang G H, Wei G H. 2024. Global turnover of soil mineral-associated and particulate organic carbon. Nat Commun, 15: 5329

Zhu Z, Woodcock C E. 2012. Object-based cloud and cloud shadow detection in Landsat imagery. Remote Sens Environ, 118: 83–94

Zhu Z, Zhang J X, Yang Z Q, Aljaddani A H, Cohen W B, Qiu S, Zhou C L. 2020. Continuous monitoring of land disturbance based on Landsat time series. Remote Sens Environ, 238: 111116

(Editorial handling: Jinzhi DING)